

Analysis of biomolecule detection with optofluidic ring resonator sensors

Hongying Zhu¹, Ian M. White¹, Jonathan D. Suter¹, Paul S. Dale², and Xudong Fan^{1,*}

¹Biological Engineering Department, University of Missouri – Columbia
240D Bond Life Sciences Center, 1201 E. Rollins Street, Columbia, MO 65211

²Ellis Fischel Cancer Center, University of Missouri – Columbia, Columbia, MO 65211

fanxud@missouri.edu

<http://web.missouri.edu/~fanxud/>

Abstract: We theoretically and experimentally analyze the biomolecule detection capability of the liquid core optical ring resonator (LCORR) as a label-free bio/chemical sensor. We first establish a simple and general linear relationship between the LCORR's bulk refractive index sensitivity (BRIS) and its response to molecule deposition onto the surface, which enables us to easily characterize the LCORR sensing performance. Then, biosensing experiments are performed with bovine serum albumin (BSA) and LCORRs of various BRISs. The experimental results are in good agreement with the theoretical prediction. Further analysis shows that the LCORR is capable of detecting BSA below 10 pM with sub-picogram/mm² mass detection limit.

©2007 Optical Society of America

OCIS codes: (230.5750) Resonators; (170.4520) Optical confinement and manipulation; (300.6490) Spectroscopy, surface; (120.1880) Detection.

References and links

1. A. Serpenguzel, S. Arnold, and G. Griffel, "Excitation of resonances of microspheres on an optical fiber," *Opt. Lett.* **20**, 654-656 (1995).
2. F. Vollmer, D. Braun, A. Libchaber, M. Khoshshima, I. Teraoka, and S. Arnold, "Protein detection by optical shift of a resonant microcavity," *App. Phys. Lett.* **80**, 4057-4059 (2002).
3. S. Arnold, M. Khoshshima, I. Teraoka, S. Holler, and F. Vollmer, "Shift of whispering-gallery modes in microspheres by protein adsorption," *Opt. Lett.* **28**, 272-274 (2003).
4. I. Teraoka, S. Arnold, and F. Vollmer, "Perturbation approach to resonance shifts of whispering-gallery modes in a dielectric microsphere as a probe of a surrounding medium," *J. Opt. Soc. Am. B* **20**, 1937-1947 (2003).
5. N. M. Hanumegowda, C. J. Stica, B. C. Patel, I. M. White, and X. Fan, "Refractometric sensors based on microsphere resonators," *Appl. Phys. Lett.* **87**, 201107 (2005).
6. I. M. White, N. M. Hanumegowda, and X. Fan, "Subfemtomole detection of small molecules with microsphere sensors," *Opt. Lett.* **30**, 3189-3191 (2005).
7. N. M. Hanumegowda, I. M. White, H. Oveys, and X. Fan, "Label-Free Protease Sensors Based on Optical Microsphere Resonators," *Sensors Lett.* **3**, 315-319 (2005).
8. I. M. White, H. Oveys, and X. Fan, "Liquid Core Optical Ring Resonator Sensors," *Opt. Lett.* **31**, 1319-1321 (2006).
9. X. Fan, I. M. White, H. Zhu, J. D. Suter, and H. Oveys, "Overview of novel integrated optical ring resonator bio/chemical sensors," *Proc. SPIE* **6452**, 6452M (2007).
10. A. Yalcin, K. C. Papat, O. C. Aldridge, T. A. Desai, J. Hryniewicz, N. Chbouki, B. E. Little, O. King, V. Van, S. Chu, D. Gill, M. Anthes-Washburn, M. S. Unlu, and B. B. Goldberg, "Optical Sensing of Biomolecules Using Microring Resonators," *IEEE J. Sel. Top. Quantum Electron.* **12**, 148-155 (2006).
11. A. M. Armani and K. J. Vahala, "Heavy water detection using ultra-high-Q microcavities," *Opt. Lett.* **31**, 1896-1898, 2006.
12. C.-Y. Chao, W. Fung, and L. J. Guo, "Polymer microring resonators for biochemical sensing applications," *IEEE J. Sel. Top. Quantum Electron.* **12**, 134-142, 2006.
13. A. Ksendzov and Y. Lin, "Integrated optics ring-resonator sensors for protein detection," *Opt. Lett.* **30**, 3344-3346 (2005).
14. R. K. Chang and A. J. Campillo, *Optical Processes in Microcavities* (World Scientific, Singapore, 1996).
15. M. L. Gorodetsky, A. A. Savchenkov, and V. S. Ilchenko, "Ultimate Q of optical microsphere resonators," *Opt. Lett.* **21**, 453-455 (1996).

1. Introduction

Optical ring resonators have recently been under intensive investigation for label-free sensor development [1-13]. In a ring resonator, the whispering gallery modes (WGMs) form due to total internal reflection of the light along the curved boundary between the high and low refractive index (RI) media [14]. The WGM is the surface mode and has the evanescent field extending into the low RI medium, thus enabling interaction with the analyte near the ring resonator surface. The WGMs have high Q-factors, making the ring resonator equivalent to a few centimeters of straight waveguide of the same evanescent light fraction, despite the small ring size [14,15]. Therefore, as compared to waveguides, the ring resonators can potentially achieve higher integration density and smaller sample consumption. The liquid core optical ring resonator (LCORR) is a unique type of ring resonator introduced recently [8,9]. The LCORR utilizes a thin-walled micro-sized capillary. As illustrated in Fig. 1, the circular cross section of the capillary forms the ring and supports the WGM. The capillary wall is sufficiently thin ($< 4 \mu\text{m}$) so that the WGMs of high Q-factors ($> 10^6$) are exposed to the core and interact with the analyte in proximity of the capillary inner surface. The LCORR takes advantage of the excellent fluidic handling capabilities of the capillaries and all the photonic sensing merits of the ring resonators, and is a promising technology platform for the next generation of micro total analysis system [9].

The LCORR, like all other ring resonator label-free sensors, essentially measures the WGM spectral response to the RI change near its sensing surface. The RI change can occur over the range either much longer or much shorter than the WGM evanescent field decay length [4]. The former is called bulk RI change and can be induced when the solution is modified [5], whereas the latter results from the deposition of molecules to the ring resonator surface [2,3,9]. The ring resonator sensing performance can be characterized by its bulk RI sensitivity (BRIS), or by the sensitivity to molecules on the sensing surface. The measurement of the BRIS is easy to implement and is non-invasive. Typically, it involves delivering the liquid of various RIs to the ring resonator and the sensing surface is subsequently regenerated by simply rinsing the test liquid off. Therefore, the BRIS can be used routinely for sensor characterization. Previously, the bulk RI detection of the LCORR has been demonstrated and the dependence of the BRIS on various parameters, such as the wall thickness, LCORR diameter, and operating wavelength, has been theoretically investigated [9].

In contrast, molecule surface density is quite difficult to characterize. It requires detailed control of the surface bio/chemical conditions for biomolecules to bind efficiently to the sensor surface. Furthermore, after characterization, relatively harsh chemicals are needed to remove those test molecules before the sensor can be used for actual biomolecule detection, which may lead to degraded surface, hence, deteriorated sensing performance. Consequently,

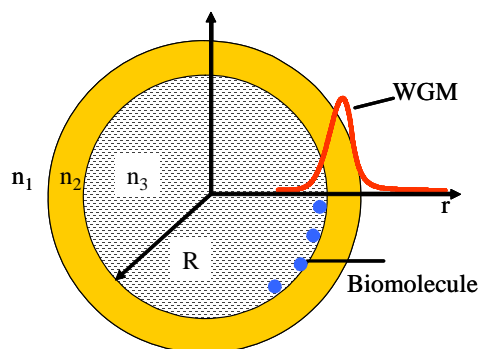


Fig. 1. Structure of the LCORR. $\epsilon_1 = n_1^2$, $\epsilon_2 = n_2^2$, $\epsilon_3 = n_3^2$ dielectric constant for surrounding medium, wall, and core. R: LCORR inner radius.

relating the BRIS of a ring resonator to the molecule binding sensitivity is of critical importance to expedite the development and characterization of ring resonator sensors. Arnold *et al.* [3] and Teraoka *et al.* [4] recently used the first-order perturbation theory to analyze the WGM spectral shift when the bulk RI changes outside a microsphere and when molecules bind to the sphere outer surface. Although these results provide excellent study of the interaction between the microsphere and the surrounding medium, they are complicated and may not be readily extended into the LCORR and other types of ring resonator sensors.

In this paper, we develop a simple model to establish a relationship between the BRIS and the molecule binding sensitivity. It is found that the WGM spectral shift for the molecules attached on the surface depends linearly on the LCORR's BRIS and the molecule density on the surface. We then apply this theory to actual LCORRs of various BRISs to analyze their biomolecule detection capability. We show that the experimental results agree well with the theoretical predication and that the LCORR is capable of detecting BSA below 10 pM with sub-pg/mm² mass detection limit. The detection and quantification of proteolytic activities are also demonstrated with trypsin, which removes molecules from the surface.

2. Theory

The LCORR structure and the relevant parameters are given in Fig. 1. The LCORR relies on the light in the core for the detection of the bulk RI change and molecule binding. Therefore, it is intuitive to calculate the fraction of the light energy in the core and use it as a central parameter that connects the BRIS and molecule binding sensitivity.

The WGM resonant wavelength, λ , can be written as:

$$2\pi R \cdot [n_1\eta_1 + n_3\eta_3 + n_2(1 - \eta_1 - \eta_3)] \approx l \cdot \lambda, \quad (1)$$

where η_1 and η_3 are the fraction of the light energy in the surrounding medium and the core, respectively. l is an integer related to the WGM angular momentum. Taking the derivative of Eq. (1), we arrive at the relation between the BRIS, S , and η_3 :

$$S = \left(\frac{\delta\lambda}{\delta n_3} \right) \approx \frac{2\pi R}{l} \eta_3 \approx \frac{\lambda}{n_2} \eta_3, \quad (2)$$

where we have used $l = 2\pi n_2 R / \lambda$, since the predominant fraction of the light is confined in the LCORR wall. Note that in derivation of Eq. (2), we have ignored the redistribution of the light, *i.e.*, the change of η_1 and η_3 , when n_3 changes. Although this seems to be a rough approximation, Eq. (2) turns out to be quite accurate, as discussed later.

The electric field decays exponentially in the core. Therefore, η_3 can be calculated as:

$$\eta_3 = \frac{2\pi h \times \int_0^R \epsilon_0 \epsilon_3 |E_0|^2 \cdot e^{-(R-r)/L} r dr}{\int \epsilon_0 \epsilon(r) \cdot |E(r)|^2 dV} \approx \frac{2\pi R h \epsilon_0 n_3^2 |E_0|^2 L}{\int \epsilon_0 \epsilon(r) \cdot |E(r)|^2 dV}, \quad (3)$$

where E_0 is the electric field at the LCORR inner surface and h is an arbitrary length along the LCORR longitudinal direction. Integration in the denominator is taken over the whole space. L is the light intensity decay constant and can be approximated by:

$$L = \frac{\lambda}{4\pi} \frac{1}{\sqrt{n_2^2 - n_3^2}}. \quad (4)$$

In Eq. (3), we assume $R \gg L$, since R/L is about 10^2 - 10^3 in all LCORRs of interest. The WGM response to the attachment of molecules to the LCORR surface, $\delta\lambda$, is calculated by using the equation developed by Arnold *et al.* in Ref. [3] and by considering Eqs. (1)-(4):

$$\frac{\delta\lambda}{\lambda} = \frac{\sigma_p \alpha_{ex} \cdot 2\pi R h \cdot |E_0|^2}{2 \int \epsilon_0 \mathcal{E}(r) \cdot |E(r)|^2 dV} = \sigma_p \alpha_{ex} \frac{2\pi \sqrt{n_2^2 - n_3^2}}{\epsilon_0 \lambda^2} \frac{n_2}{n_3} S, \quad (5)$$

where σ_p is the biomolecule surface density and α_{ex} is the excess polarizability of the molecule.

Eq. (5) indicates that the WGM spectral shift for molecule attachment is linearly proportional to the LCORR BRIS and to the molecule surface density. In addition, the contribution of each molecule to the WGM shift is weighted by the LCORR BRIS. Using Eq. (5), the molecule detection limit, σ_{min} , can also be deduced:

$$\sigma_{min} = \left(\frac{n_3^2}{n_2 \sqrt{n_2^2 - n_3^2}} \frac{\epsilon_0 \lambda}{2\pi \alpha_{ex}} \right) \Delta_{min}, \quad (6)$$

where Δ_{min} is the bulk RI detection limit in units of RIU.

To verify Eq. (2), we use the in-house simulation codes based on the three-layer Mie theory [8] to calculate the BRIS (S_{sim}) and the η 's. Table 1 compares S_{sim} with S_{est} estimated using Eq. (2), when bulk RI sensing occurs either in the core or outside the LCORR. The fraction of light is varied from less than one percent to nearly fifty percent; and S_{est} matches S_{sim} within a few percent. Note that Eq. (2) is also valid when η becomes 0 or 1.0, which corresponds to the scenario that no light or the whole ring resonator is utilized for RI sensing.

Table 1. Comparison between S_{sim} and S_{est} . $n_2 = 1.45$.

λ (nm)	960.797		968.605		979.169	
η	0.455% (η_1)	0.288% (η_3)	1.06% (η_3)	5.628% (η_3)	1.582% (η_1)	41.87% (η_3)
S_{sim} (nm/RIU)	3.11	1.86	7.07	37.1	11.5	288
S_{est} (nm/RIU)	3.01	1.91	7.08	37.6	10.7	283

It should be emphasized that although Eq. (5) is developed under the framework of the LCORR, it is generally applicable to other types of ring resonator sensors, no matter whether inner or outer surface is used for sensing and regardless of the mode number and polarization. For example, for a microsphere, the BRIS for TE mode is approximately [4,5]:

$$S \approx \frac{\lambda^2 n_1}{2\pi R \sqrt{(n_2^2 - n_1^2)^3}}. \quad (7)$$

Therefore, the WGM spectral shift in response to the molecule attachment onto the microsphere surface is:

$$\frac{\delta\lambda}{\lambda} = \left(\frac{\sigma_p \alpha_{ex}}{\epsilon_0 R} \frac{1}{n_2^2 - n_1^2} \right) \frac{n_2}{n_1}. \quad (8)$$

The term in the parenthesis is the same as what Arnold *et al.* reported in Ref. [3]. For $n_1 = 1.33$ and $n_2 = 1.45$, the factor n_2/n_1 will lead to a 10% difference between our results and Arnold's.

3. Experimental results

We now utilize the theory developed in the previous section to analyze the LCORR biomolecule detection capability. The LCORRs are fabricated using the method described in Ref. [8,9]. A 980 nm tunable diode laser is coupled into the WGM of the LCORR via an

optical fiber taper in touch with it. The laser is scanned in wavelength and the resonant dip indicating the WGM spectral position is monitored at the taper output.

First, we measure the LCORR BRIS. The LCORR is initially filled with 18-M Ω water and then various concentrations water-ethanol mixtures with known RI are passed sequentially through the LCORR. The WGM shifts to a longer wavelength in response to the RI increase in the core, as illustrated in the inset of Fig. 2. The sensitivity in Fig. 2 is obtained by calculating the slope of the WGM response to the RI change [8,9]. After the BRIS characterization, the LCORR is rinsed with 18-M Ω water and silanized with 1% 3-aminopropyltriethoxysilane in water, followed by treatment of 5% glutaraldehyde for 20 minutes and thorough rinsing with water. Finally the LCORR is filled with PBS buffer and ready for protein detection.

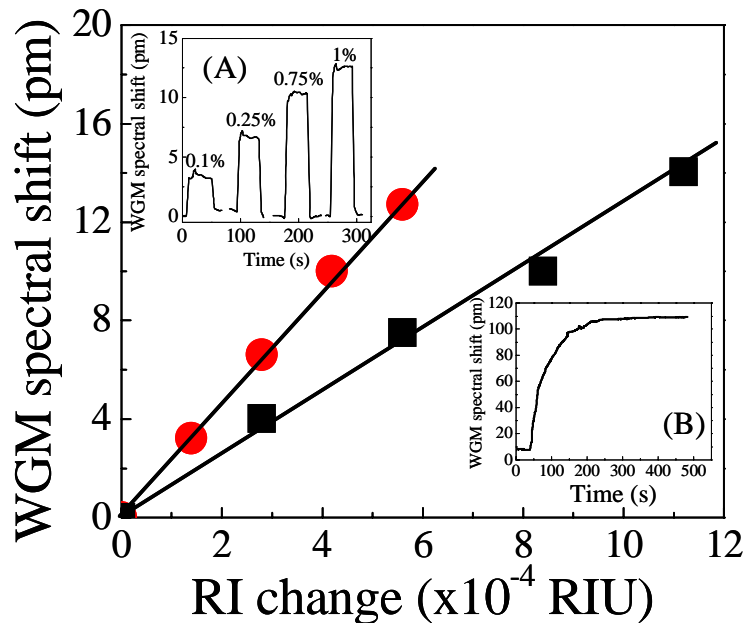


Fig. 2. Two representative BRIS curves of the LCORRs used in experiment. Solid curves are linear fits. Inset (A): Response of the LCORR to various concentrations of water-ethanol mixtures. (B): Response of the LCORR to BSA binding to the surface.

Bovine serum albumin (BSA, molecular weight: 66 kD) prepared in the PBS buffer is then pumped through the LCORR. We start with the lowest concentration and gradually increase the BSA concentration. For each BSA concentration, the WGM spectral position shifts quickly to a longer wavelength and then levels off, indicating that the equilibrium is reached between the BSA molecules in solution and on the LCORR surface, as shown in Inset (B) in Fig. 2. Figure 3 plots the equilibrium WGM shift vs. BSA concentration for one of the LCORRs under test. With the increased BSA concentration, the equilibrium WGM shift increases and then becomes saturated when BSA concentration is higher than 200 nM.

The same experiment is repeated for LCORRs of various BRISs. In Fig. 4, the saturation WGM shift is plotted against the LCORR BRIS. Also plotted is the theoretical curve based on Eq. (5) using the excess polarizability provided in Ref. [3] and assuming that the surface is fully covered by BSA molecules. Nearly all experimental data in Fig. 4 are very close to this

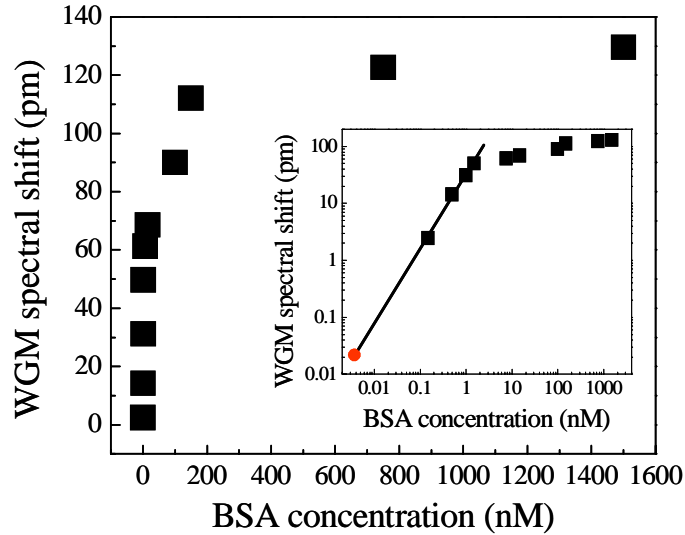


Fig. 3. WGM spectral shift vs. BSA concentration for the LCORR with BRIS of 31 nm/RIU. The LCORR starts to saturate at 200 nM and the saturation WGM shift is 129 pm. Half saturation concentration: 8 nM. Inset: log-log scale. Solid line is the linear fit in log-log scale. Red dot: detection limit for BSA concentration.

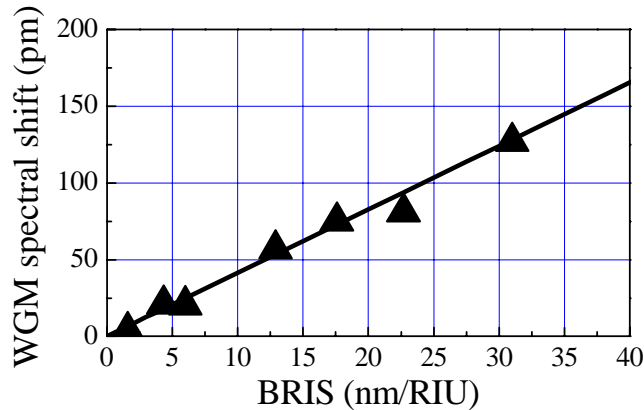


Fig. 4. Saturation WGM spectral shift vs. LCORR BRIS. The solid curve is the theoretical calculation based on Eq. (5). $n_2 = 1.45$, $n_3 = 1.333$. $\sigma_p = 2.9 \times 10^{12} \text{ cm}^{-2}$ and $\alpha_{ex} = (4\pi\epsilon_0)(3.85 \times 10^{-21}) \text{ cm}^3$ are obtained from Ref. [3].

theoretical curve, suggesting that BSA forms a very compact layer on the LCORR surface, in agreement with previous observations [2,3,7].

The results obtained above provide a mechanism to estimate the LCORR biomolecule detection limit. It is known that the spectral resolution of the WGM detection is limited by the Q-factor and temperature fluctuations [9,16]. For $Q \sim 10^6$, the WGM noise caused by temperature fluctuations becomes a dominant factor. With a thermo-electric cooler, the WGM noise (3 standard deviation) on the order of 0.02 pm has been achieved [9]. Therefore, for the LCORR with a BRIS of 31 nm/RIU, the bulk RI detection limit is 6×10^{-7} RIU, which, according to Eq. (6), corresponds to a BSA mass detection limit of 0.5 pg/mm^2 . For an LCORR of $100 \text{ }\mu\text{m}$ in diameter with the WGM extension along the LCORR of $10 \text{ }\mu\text{m}$ [9], the minimal detectable mass is 1.5 fg.

From an experimental point of view, it is also important to characterize the LCORR detection limit in terms of sample concentration, which, in conjunction with the molecule binding affinity, determines the amount of molecules bound to the surface: $f = [BSA]/(K_d + [BSA])$, where f is the fraction of the sites on the surface occupied by BSA, $[BSA]$ is the BSA concentration in solution, and K_d is the dissociation constant. In the limit of the low BSA concentration, the WGM spectral shift should have the following BSA concentration dependence: $\log(\delta\lambda) \sim \log([BSA])$. The inset of Fig. 3 shows the LCORR curve indeed follows this dependence. The detection limit obtained by extrapolation is estimated to be approximately 3 pM, reflecting the excellent detection capability of the LCORR. In fact, the lowest concentration used in Fig. 3 is 0.15 nM, causing a spectral shift of 2.5 pm, well above the LCORR detection noise level. For a comparison, 0.3 nM avidin, a protein similar to BSA, has previously been detected with a large (2 mm diameter) ring resonator; the detection limit of 0.1 nM is deduced [13]. Note that the slope of the WGM shift curve in the inset of Fig. 3 is not unity at low BSA concentrations, reflecting the random adsorption of BSA molecules onto the surface, in contrast to antigen-antibody type binding with a defined binding ratio.

In addition to detecting the addition of biomolecules, the LCORR is also capable of detecting molecules removed from the surface, which is important for measurement of enzyme proteolytic activities. Figure 5 shows that amino acids are cleaved from BSA on the LCORR surface by trypsin. Initially, a high concentration of BSA is used to ensure that the surface is fully covered, which is verified by the theoretical curve in Fig. 4. Upon the injection of trypsin, the WGM shifts to a lower wavelength, corresponding to a mass reduction on the surface, from which the mass removal rate or trypsin proteolytic activity can be deduced [7]. Figure 5 shows that 80% of BSA molecules are removed from the LCORR. The remaining 20% will permanently remain on the LCORR surface due to the lack of available cleavage sites, consistent with the result obtained previously with microspheres [7].

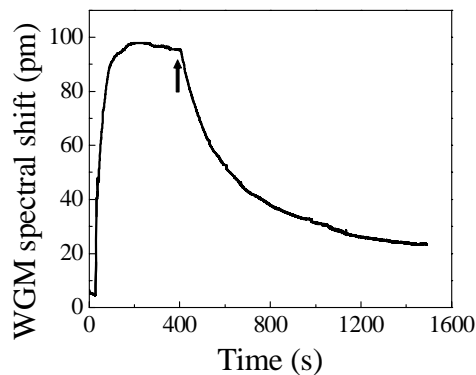


Fig. 5. BSA molecules bind to the LCORR surface, followed by the cleavage by trypsin. BSA concentration: 0.1 mg/mL. Trypsin concentration: 0.1 mg/mL. Arrow indicates the time when trypsin is added.

4. Summary

We have developed a simple and general formula relating the ring resonator BRIS with its molecule binding sensitivity. Applying this formula, we have analyzed the biomolecule detection capability of the LCORR. Both theoretical and experimental agree quite well. Furthermore, we have shown the detection limit of protein is sub-pg/mm².

Our work has numerous applications in development of the LCORRs and other types of ring resonators. It provides an easy, non-invasive, standardized way to quantitatively predict the ring resonators' sensitivity to biomolecules. It becomes particularly useful when immobilization of biorecognition molecules with controlled density is needed, and when the actual molecule mass on the ring resonator surface needs to be measured.

Acknowledgments

The authors acknowledge the support from the 3M Non-Tenured Faculty Award, the Wallace H. Coulter Early Career Award, and Petroleum Research Fund (43879 -G 10).